Chapter 2
Active Layer Materials for Organic Solar Cells

Jianhui Hou and Xia Guo

Abstract Organic photovoltaic cell (OPV) has emerged as a new competitor to inorganic material-based solar cells, due to its potential application in large area, printable, and flexible solar panels. In particular, OPV cells with bulk heterojunction architecture (BHJ), in which the photoactive layer consists of a bicontinuous blend of an electron donor and an electron acceptor, has allowed power conversion efficiencies (PCEs) over 8 %. Electron donor and electron acceptor materials, with ideal properties are requisite for reaching high PCE. In this chapter, the relationship between molecular structure and photovoltaic property of active layer materials will be discussed, and also the rules of molecular design of organic photovoltaic materials will be presented. Furthermore, the latest progresses of electron donors and electron acceptors, especially for conjugated polymers and the fullerene derivatives, will be introduced.

2.1 Introduction

An Organic photovoltaic cell (OPV) cell is composed of a film of organic photovoltaic active layer, sandwiched between a transparent electrode and a metal electrode. As a successful branch of OPV, polymer solar cells (PSCs) have attracted much attention. Typically, the active layer PSC device is composed of a blend film of conjugated polymer (as electron donor) and a small molecular acceptor. The conjugated polymer donor and the fullerene derivative acceptor are

J. Hou (✉) · X. Guo
State Key Laboratory of Polymer Physics and Chemistry, Beijing National Laboratory for Molecular Sciences, Institute of Chemistry, Chinese Academy of Sciences, Beijing 100190, China
e-mail: hjhzlz@iccas.ac.cn

W. C. H. Choy (ed.), *Organic Solar Cells*, Green Energy and Technology,
DOI: 10.1007/978-1-4471-4823-4_2,

the key photovoltaic materials for high performance PSCs, and therefore, what are ideal properties and how to get photovoltaic materials with ideal properties are of great importance to photovoltaic materials design.

Bulk heterojunction (BHJ) structure is the most successful structure invented by Yu et al. [1], in which a blend of donor and acceptor with a bicontinual phase separation can be formed. When the sunlight getting through the transparent electrode is absorbed by the semiconducting donor and acceptor materials in the photoactive layer, excitons (bounded electron–hole pairs) are formed, and then the excitons diffuse to the interfaces of the donor/acceptor where the excitons dissociate into electrons on the LUMO level of the acceptor and holes on the HOMO level of the donor. The dissociated electrons and holes are driven by build-in electric field and then moved to negative and positive electrode, respectively, and then collected by the electrodes to realize the photon-to-electron conversion.

Figure 2.1 shows the electronic energy levels of the donor and acceptor in a P3HT/PCBM blend system. The absorption band of P3HT/PCBM covers the range from 380 to 670 nm, which means that the photons with energy between 2.0 and 3.3 eV can be absorbed by the active layer, and the excitons will be formed. In order to make better utilization of the sunlight, active layer materials with broad absorption band is required, and for this purpose, more and more low band gap (LBG) materials have been developed and great successes have been made in the past decade. Since, the LUMO and the HOMO of P3HT is higher than that of PCBM, the excitons will separate into positive and negative charges at the interface of the P3HT phase and PCBM phase. The negative charge will transport through the LUMO of PCBM and the positive charge will transport through the HOMO of P3HT, and then the charges can be collected by the electrodes. In order

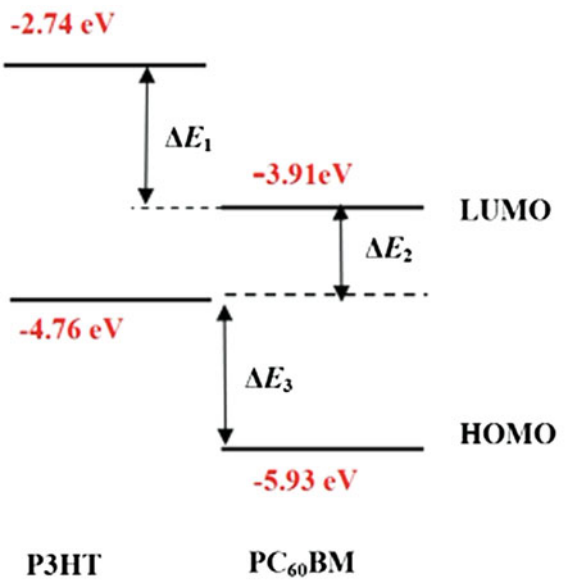

Fig. 2.1 Electronic energy level of P3HT and $PC_{60}BM$

to get efficient charge separation, HOMO and LUMO of the donor material should be 0.2–0.3 eV higher than that of the acceptor material, respectively. If the offset is too small, it would be hard to get efficient charge separation; if the offset is too big, much energy loss would be happened. As known, open-circuit voltage (V_{oc}) of BHJ OPV devices are directly proportional to the gap between HOMO of the donor and LUMO of the acceptor [2]. Although, the energy of the photon that can be utilized by the P3HT/PCBM system is higher than 2.0 eV, V_{oc} of P3HT/PCBM-based OPV device is typically around 0.6 eV, meaning that more than 70 % energy loss is taking place during the photoelectric conversion process. Therefore, to minimize the energy loss, HOMO and LUMO levels of the donors and the acceptors should be tuned carefully.

Furthermore, mobility of the donor and the acceptor materials is also an important issue for organic photovoltaic materials. In comparison with inorganic semiconductors, organic semiconducting materials exhibit much lower mobility, and therefore, how to improve hole or electron mobility of organic photovoltaic materials becomes one of the critical objectives of molecular design of materials. For an organic semiconducting material, both inter- and intra-molecular charge transfer properties are very important. The relationship between intra-molecular charge transfer property and molecular structure is still unclear. To enhance inter-molecular stacking properties has been proven to be an effective way, to improve inter-molecular charge transportation. For examples, the hole mobility of regio-regular P3HT is 2–3 orders higher than regioregular P3HT due to the stronger pi–pi stacking property of the former [3]; to reduce the steric hindrance caused by non-conjugated side chains is also an useful approach to improve the inter-chain pi–pi stacking property of organic semiconducting materials and hence higher mobility can be realized [4].

Besides absorption band, molecular energy levels (HOMO and LUMO), and mobility, there are still many other issues like solubility in different solvents and chemical stability, should be considered in molecular design of organic photovoltaic materials. Therefore, how to balance these properties is the key to get an organic photovoltaic material with ideal properties. Herein, several broadly used material systems will be introduced in this chapter to provide a general profile of molecular structure design of organic photovoltaic materials.

Poly(phenylene vinylene)s (PPV) and Polythiophenes (PTs) are two kinds of classic conjugated polymers which are broadly used in photovoltaic cells and light emitting diodes. MEH-PPV [5] and MDMO-PPV [6], as shown in Scheme 2.1 are two representatives of PPV-based materials. These two PPVs can be used as electron donor materials in solar cells, and they exhibited much similar photovoltaic properties. PCE of $\sim$2 % has been recorded by using MEH-PPV/PCBM-based solar cells. However, the absorption edges of MEH-PPV and MDMO-PPV are at about 550 nm, corresponding to a band gap of ca. 2.3 eV, and output current density of the solar cells based on them was limited due to the big mismatch between their absorption spectra and the solar irradiation spectrum. In comparison with MEH-PPV and MDMO-PPV, P3HT, one of the derivative of poly(3-alkyl-thiophene) exhibits lower band gap, broader absorption band and also better hole

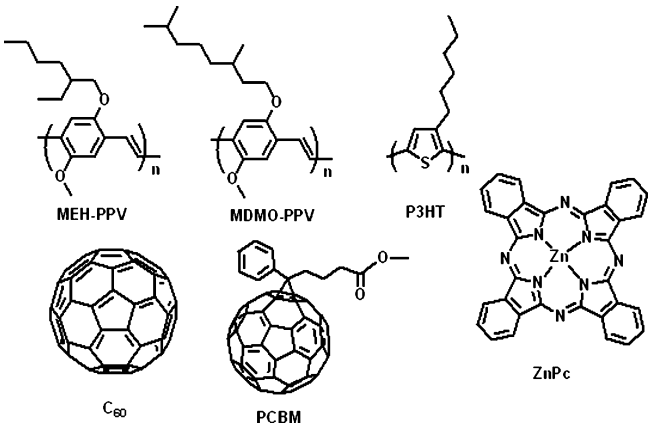

Scheme 2.1 Molecular structures of several representative organic photovoltaic materials

mobility, and therefore, this conjugated polymer exhibited much better photovoltaic properties. By using P3HT as donor material blending with PCBM as acceptor, over 4 % PCE has been well repeated by different research groups, and P3HT has attracted much attention in the OPV filed. Interestingly, photovoltaic properties of P3HT/PCBM system are very sensitive to the morphology of the blend, therefore, morphology study of this system has been well investigated. For example, by using annealing [7], post-annealing [8] or solvent annealing process [9], slow-growth process [10], additives [11], the morphology of the blend can be well controlled and thus photovoltaic performance of the P3HT/PCBM system can be improved. Small molecular organic semiconductors with appropriate properties can also be used as electron donor materials in OPV devices. ZnPc is one of the successful examples. Unlike conjugated polymers, ZnPc has poor solubility in commonly used solvents, thus thermal evaporation method under high vacuum is used to make ZnPc-based solar cells.

Fullerene and its derivatives are broadly used as electron acceptor materials in OPVs. The solubility of unsubstituted fullerene is quite poor, which limits its application in device fabrication process. Therefore, different substituents were introduced onto fullerene. In 1995, Hummelen and Wudl et al. reported a feasible approach to synthesize PCBM ([6,6]-phenyl-C61-butyric acid methyl ester), one of the most successful fullerene derivative, which exhibits excellent photovoltaic properties as electron acceptor material.

Although, $\sim$8 % PCEs have been achieved, efficiency of OPVs is still much lower than inorganic photovoltaic cells. New organic materials with ideal properties are still requisite. Therefore, in the following section, OPV materials will be sorted into different groups based on functions (donor and acceptor) and molecular structures to give a sketch of the relationship between molecular structures and photovoltaic properties.

2.1.1 Band Gap and Molecular Energy Level Control

Polymers, oligomers, and small molecular compounds with conjugated backbones can be used as electron donor material in OPV devices. Although, these three categories of compounds are different, as photovoltaic donor materials, the requirements for their properties are quite similar. Broad absorption bands and appropriate molecular energy levels are first required, and also the strategies used to modulate absorption bands, and molecular energy levels of polymers, oligomers, and small molecular compounds are similar. In this section, conjugated polymers will be used as examples. Band gap (Eg) of conjugated polymer based on the absorption edge obtained at long wavelength direction (Eg = 1240/λedge) is used as a ruler to evaluate the absorption band of conjugated polymers. In order to utilize more sunlight, absorption edge of conjugated polymer should be extended to near-infrared region. Therefore, to find efficient way to lower band gap of conjugated polymer is crucial to molecular design. As known, the band gap and the molecular energy levels (HOMO and LUMO) of a conjugated polymer is closely related to the molecular weight, molecular configuration and conformation, intermolecular interaction, effective conjugating length, and so on, and most of LBG polymers were designed based on these parameters.

Two strategies are well used in molecular design of LBG polymer. To make a conjugated structure with enhanced quinoid structure is an effective way to get LBG material. When a quinoid structure is formed, the conjugation of the backbone will be enhanced and the pi-electrons will be more delocalized, and hence the polymer's band gap will be lowered greatly. For example, molecular structure of 2,1,3-benzothiadiazole (BT) is similar as that of thieno[3,4-b]pyrazine (TPZ) (see Scheme 2.2), but these two components exhibited much different influence on band gaps of conjugated polymers. When TPZ is copolymerized with a conjugated building block, band gap of the resulting polymer is much lower than that of BT-based polymer. For instance, the onset of the absorption spectrum of the alternating copolymer of benzo[1,2-b:4,5-b′]dithiophene (BDT) and BT (PBDTBT in Scheme 2.2) was at $\sim$700 nm, corresponding to a Eg of 1.7 eV; however, the onset of the absorption spectrum of PBDTTPZ was at $\sim$1000 nm, corresponding to a Eg of 1.2 eV. As shown in Scheme 2.2, BT and TPZ are formed by a five-member ring fused with a six-member ring. For PBDTBT, the polymerization was taken place on 4 and 7 positions on the five-member ring of the BT unit; and for PBDTTPZ, the polymerization was taken place on 5 and 7 positions on the six-member ring of the TPZ unit. The quinoid structure of the polymer PBDTTPZ can be stabilized by the six-member ring of the TPZ units, and thus to form a more stable aromatic electron structure for the six-member ring, whereas the electron structure of the five-member ring of BT has no change in its aromatic and quinoid structures. Based on this scheme, it can be seen that the six-member ring of TPZ will stabilize the quinoid structure of the conjugated backbone of the polymer better than the five-member ring of BT, and thus a more stable quinoid structure will be formed in polymer PBDTPTZ than in PBDTBT. Since, the quinoid form

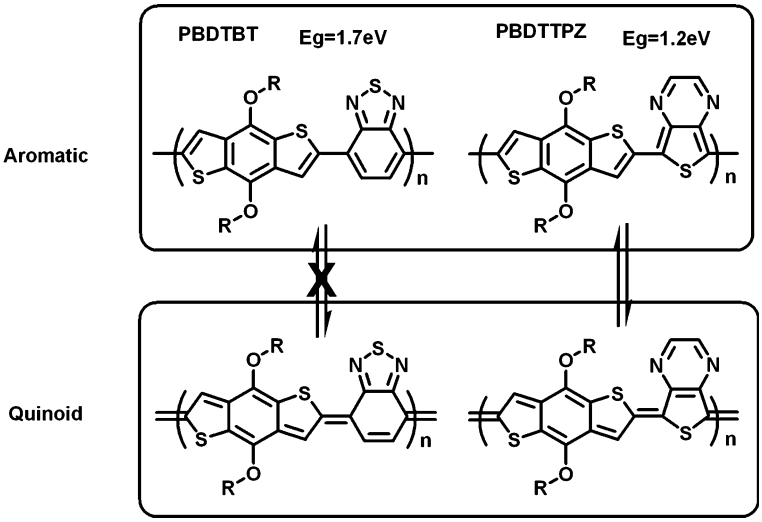

Scheme 2.2 Aromatic and quinoid forms of two conjugated polymers, PBDTBT and PBDTTPZ

has a smaller band gap than the aromatic form [12], the band gap of PBDTTPZ is lower than that of PBDTBT. Besides of TPZ unit, several other conjugated components and their derivatives with strong quinoid characteristics, as shown in Scheme 2.3, can also be used in LBG polymers.

To build a conjugated structure with alternative electron donor and electron acceptor units (D/A structure) is another effective approach to get LBG polymer. Many LBG polymers for solar cells were successfully designed based on this method, but it is still hard to get an exact theoretical calculation for the band gap of a newly designed conjugated structure. As known, the enhanced intra-molecular charge transfer is helpful to get a broadened valance and conducting bands, and hence lower band gap of a conjugated polymer with D/A structure can be reduced by increasing electron donating effect of the electron donor units or by increasing electron withdrawing effect of the electron acceptor units; the band gap of conjugated polymer with D/A structure is also tunable by changing the ratio of the donor and acceptor moieties in the polymer backbone.

2.1.2 Molecular Energy Level

As discussed above, performance of an OPV device is closely related to molecular energy levels of its active layer materials. Therefore, how to modulate HOMO and

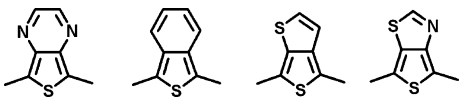

Scheme 2.3 Several aromatic building blocks that can form stable quinoid structures

LUMO levels of active layer materials are very important issue for molecular design. For organic semiconductors, HOMO and LUMO can be tuned by modifying their backbones or side groups. Poly(*p*-phenylene) (PPP) and its derivatives, like polyfluorene (PF), are not electron-rich materials, and hence HOMO levels of this kind of polymers are quite low (typically below −5.3 eV); polymers or oligomers built by electron-rich conjugated components, like thiophene or pyrrole, exhibit much strong electron donating property and hence high HOMO levels. Side groups (substituents on the backbones) have great influence on molecular energy levels of organic semiconductors. The comparison of molecular energy levels of PBDTTT-E, PBDTTT-C, PBDTTT-CF, and PBDTTT-S provides a good example for the effect of side groups. As shown in Scheme 2.4, these four polymers have identical conjugated backbones and different side groups. The basic properties of these four polymers are shown in Table 2.1. From PBDTTT-E to PBDTTT-S, the electron withdrawing effect of side groups were increased stepwise (electron withdrawing effect: ester < carbonyl < carbonyl + F < sulfonyl), and therefore, the HOMO and LUMO levels were gradually lowered.

2.1.3 Mobility Improvement

To improve mobility of an organic semiconductor is a more complicated task, than to modulate its band gap and molecular energy level. In order to get good mobility, several issues should be considered during molecular structure design. Inorganic semiconductors have well-defined crystalline structure and the charges (hole or electron) can be transported easily through the conduction band; for organic semiconductor, the charges are localized due to their low dielectric constants. Therefore, organic semiconductors have much lower mobilities than inorganic semiconductors. Since, the molecules of an organic semiconductor are stacked together by weak forces, like van der Waals force, and the charges are transported through a hopping mode, compact stacking is necessary to facilitate the intermolecular charge transport. For example, regioregular poly(3-alkylthiophene) shows much better hole mobility than its regioregular analog [3].

Band gap, molecular energy level, mobility, solubility, and the other issues of conjugated polymers and small molecular materials are quite susceptible to their

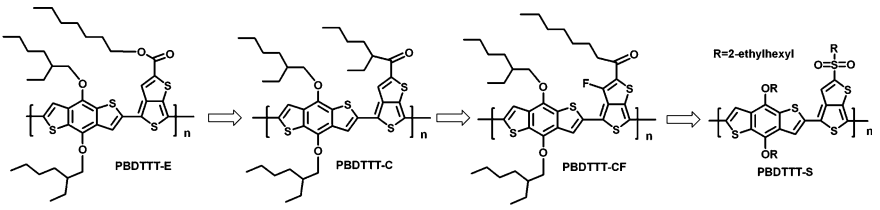

Scheme 2.4 Molecular structures of four PBDTTTs

Table 2.1 Properties and devices characteristics for the BDT-based low band gap polymers

Polymer	Eg(opt) (eV)	HOMO/LUMO (eV/eV)	J_{sc} (mA/cm^2)	V_{oc} (V)	FF	PCE (%)	Refs
PBDTTT-E	1.77	−5.01/− 3.24	13.2	0.62	0.630	5.15	[13]
PBDTTT-C	1.67	−5.12/− 3.35	14.7	0.70	0.641	6.58	[14]
PBDTTT-CF	1.77	−5.22/− 3.45	15.2	0.76	0.669	7.73	[15]
PBDTTT-S	1.63	−5.12/− 3.49	14.1	0.76	0.580	6.22	[16]

molecular structures. Since, it is hard to get a clear and exhaustive conclusion to guide molecular design of photovoltaic materials with conjugated structures, to have a comprehensive understanding of the properties of more organic photovoltaic materials would be the best way to understand the mechanisms of molecular design.

2.2 Active Layer Materials

2.2.1 Electron Donors

Numerous donor materials, including polymers and small molecular compounds, have been developed in the past decades. It is hard to categorize these materials. In this section, polythiophenes were used as an example for polymer materials with homoconjugated backbones; polymers with 2,1,3-benzothiadiazole, pyrrolo[3,4-c]-pyrrole-1,4-dione, and benzo[1,2-b;4,5-b′]dithiophene were used as three examples for molecular structure design of conjugated materials with D/A structures.

2.2.1.1 Polythiophene and Its Derivatives

Poly(3-alkylthiophene)s (P3AT) have been used as active material for optoelectronic devices, especially for photovoltaic cells. As mentioned above, P3HT is the best one in P3ATs as photovoltaic material. Typically, P3ATs can be synthesized easily through different methods. The repeating units of P3ATs were asymmetric, so three relative orientations are available when two thiophene rings are coupled between the 2- and 5-positions (Usually, the 2-position is called as head, and the 5-position is called as tail). So, the first of these is head-to-tail (HT) coupling, the second is head-to-head (HH) coupling, and the third is tail-to-tail (TT) coupling. As shown in Scheme 2.5, this leads to a mixture of four chemically distinct triad regioisomers when 3-substituted (or asymmetric) thiophene monomers are employed [17]. The HT–HT structure of polythiophenes are denoted as regioregular, the other three structures are denoted as regioregular or regiorandom, and

Scheme 2.5 Several polythiophene derivatives

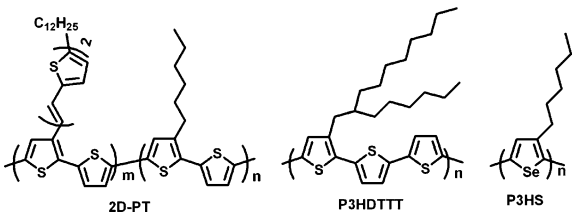

the HT–HT isomer proportion in polymers is named as regioregularity. Regioregular poly(3-substituted thiophene) can easily access a low energy planar conformation, leading to highly conjugated polymers. An increase of the torsion angles between thiophene rings leads to greater band gaps, with consequent destruction of high conductivity and other desirable properties, hence the regioregularity is an important factor in characterization of poly(3-substituted thiophene), and P3HT with high regioregularity (>98 %) is first required for high photovoltaic performance. Currently, the influence of regioregularity on photovoltaic properties of the other polymer systems has not been well studied, but this parameter would be one of the keys to do further improvement of molecular structures.

Although, P3HT exhibited promising photovoltaic properties, the absorption band (from 500 to 650 nm) of this polymer is still not broad enough to get good harvest of the sunlight. Two-dimensional conjugated polythiophenes (2D-PTs) provided a feasible way to broaden absorption band. A representative structure of 2D-PT, absorption band of 2D-PT is formed by two parts [18]. One part located at short wavelength direction is from the conjugated side chain; and another located at long wavelength direction is from the conjugated main chain. By adjusting the conjugated length of the side chain, the absorption peak position at short wavelength direction can be tuned, and by adjusting the *m*:*n* value, a broad and strong absorption band can be obtained. 2D-PTs also exhibited better hole mobilities than P3ATs, and 2 and 3 orders improvement of hole mobilities have been observed in some kinds of 2D-PTs [19].

To replace the alkyl side groups of P3ATs by alkoxy groups is an effective way to reduce the band gap of polythiophenes. Band gaps of poly(3-alkyloxythiophene)s (P3AOTs in Scheme 2.4) are ~1.55 eV, which is much lower than that of P3ATs. Although, P3AOTs have much better absorption band compared to that of P3ATs, P3AOTs are not suitable as electron donors due to their high-lying HOMO levels. Since, the alkoxy has much stronger electron donating effect than alkyl, HOMO levels of P3AOTs were ca. 0.4 eV higher than those of P3ATs. Since, the electron donating effect of side groups of polythiophenes is one of the keys to tune their HOMO levels and alkyls can be seen as weak electron donating groups, to use less alkyl substituents should be helpful to get deep HOMO level. P3HDTTT (see Scheme 2.5) was designed based on this strategy. It can be seen that for P3HT, each thiophene unit has one alkyl; for P3HDTTT, three thiophene units possess one alkyl. As a result, P3HDTTT exhibits deeper HOMO level than that of

P3HT, and thus, a V_{oc} of 0.84 V has been achieved from P3HDTTT/PCBM-based device, which is 0.24 V higher than that of P3HT/PCBM-based device [20].

Another strategy to lower the band gap of rr-P3HT was the synthesis of regioregular poly(3-hexylselenophene) (rr-P3HS). Ballantyne et al. successfully completed the synthesis of this polymer and applied it in OPVs [21]. The optical band gap (i.e., 1.60 eV) of the resulting polymer was much lower than that of the P3HT. The cells were fabricated by following similar conditions as used in P3HT-based devices, and a PCE of 2.7 % was achieved.

2.2.1.2 Polymers with 2,1,3-Benzothiadiazole

2,1,3-Benzothiadiazole (BT) has been widely used as electron deficient building block in conjugated polymers with D/A structure. This category of polymer donors has been extensively studied and showed outstanding photovoltaic performances (the performances of the copolymers are summarized in Table 2.2). As known, thiophene is a typical electron-rich unit with weak aromatic property and hence thiophene derivatives are broadly used as electron donating building blocks in conjugated polymers. Several copolymers, based on derivatives of dithiophene and BT are shown in Scheme 2.6. It can be seen that the dithiophene derivatives shown in Scheme 2.6 possess well planar structures, which were confined by the bridge atoms, like N, C, or Si, or by a planar conjugated unit.

PCPDTBT is the first low band gap polymer which was successfully synthesized and used in PSCs [22, 25]. PCPDTBT has strong and broad absorption band extending to near-infrared region, corresponding to a band gap of 1.50 eV, and this polymer also exhibited a good hole mobility, 1×10^{-3} cm^2/V s by field effect transistor (FET) [23]. Initially, the PCE of PCPDTBT/PCBM system was $\sim$3.2 % [22]. Then, the morphology of the blend was optimized by using diiodooctane (DIO) or 1,8-dithiol-octane (ODT) as additive during the spin-coating process, and hence the PCE was improved to >5 % [26]. Since, the solubility of PCBM in DIO

Table 2.2 Properties and devices characteristics for polymers of Schemes 2.6 and 2.7

Polymer	Eg(opt) (eV)	HOMO/LUMO (eV/eV)	J_{sc} (mA/cm^2)	V_{oc} (V)	FF	PCE (%)	Refs
PCPDTBT	1.40	−5.30/− 3.57	16.2	0.62	0.55	5.5	[26]
PSBTBT	1.37	N.A.	17.3	0.57	0.61	5.9	[24]
PDTPBT	1.43	−4.81/− 3.08	11.9	0.54	0.44	2.8	[30]
PFDTBT	N.A.	N.A.	7.70	1.00	0.54	4.2	[31]
PFSiDTBT	1.86	−5.70/− 3.81	9.40	0.90	0.51	5.4	[32]
PCDTBT	1.88	−5.50/− 3.60	10.6	0.88	0.66	6.1	[33]
PDTPDTBT	1.46	−5.00/− 3.43	9.47	0.52	0.44	2.2	[34]
PCPDTDTBT	1.55	N.A.	8.75	0.60	0.4	2.1	[35]
PBDTDTBT	1.75	−5.31/− 3.44	10.7	0.92	0.57	5.66	[36]
PSiDTBT	1.53	−4.99/− 3.17	10.67	0.62	0.52	3.4	[37]

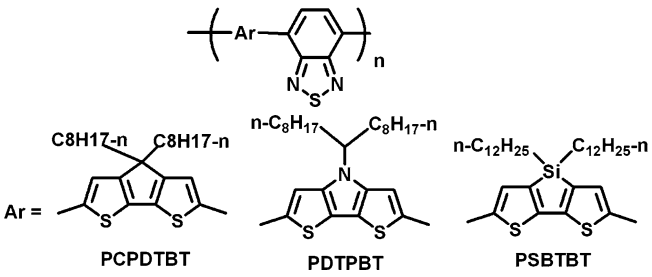

Scheme 2.6 Several representatives of BT-based polymers with D/A structure

is better than that of the polymer, and DIO has much lower vapor pressure than the commonly used solvents during device fabrication process, like *o*-dichlorobenzene (DCB) and chlorobenzene (CB), during the spin-coating process, the polymer can be crystallized or separated from the blended solution while avoiding excessive crystallization of PCBM [27]. This method has been proved to be an effective way to improve photovoltaic properties in many other polymer/PCBM systems, and a lot of good results were developed by using DIO as additive. The success of this method indicates that the morphology control of polymer/PCBM blend is of great importance to OPVs.

A silo-contained polymer, PSBTBT, with similar molecular structure as PCPDTBT was synthesized and also exhibited excellent photovoltaic properties [28]. In PSBTBT, an Si atom was introduced to the bridge point (3, 3′ positions) on the bithiophene unit. Band gap and HOMO level of PSBTBT are 1.55 eV and − 5.1 eV [29]. As mentioned above, in PCPDTBT/PCBM blend photovoltaic system, in order to optimize the morphology and hence to get higher performance, additives were necessary during the spin-coating process. For PSBTBT/PCBM blend, thermal annealing less than 140 °C for 15 min was enough to get optimized morphology of the blend. Without annealing, the PCE of PSBTBT/PCBM-based devices were ∼3.5 %; after annealing, the PCE increased to 5.6 %. However, for PCPDTBT/PCBM system, annealing had no help. The interesting phenomenon was ascribed to the difference between atom diameter values of carbon and silicon. As known, the diameter of silicon atom is 50 % bigger than that of carbon, so the bulky alkyl side chains of PCPDTBT is closer to the conjugated backbone than that of PSBTBT. The conjugated backbone of PSBTBT would stack tighter than that of PCPDTBT. Therefore, the former exhibits better hole transport property than the latter [24].

The silicon atom of PSBTBT can also be replaced by a nitrogen atom, and the polymer PDTPBT was obtained [30]. PDTPBT exhibited much lower band gap (1.4 eV) and higher HOMO level (−4.6 eV) than those of PCPDTBT and PSBTBT due to the strong electron donating effect of the amino group. Since, the HOMO level of PDTPBT was higher than the other two analogs, PDTPBT/PCBM-based solar cell exhibited a V_{oc} of ∼0.4 V, which limited its photovoltaic performance tremendously. The polymer PBDTBT exhibited a broader band gap

(1.7 eV) and deeper HOMO level (−5.3 eV) compared to PDTPBT. Although, band gap and HOMO level of PBDTBT are suitable for solar cell and V_{oc} over 0.8 V has been recorded, the photovoltaic performance of PBDTBT/PCBM blend system has not been well optimized, and PCE of this polymer was still below 2 %.

In order to develop more efficient photovoltaic materials, thiophene units were introduced to the 4- and 7-positions of BT, and an important derivative named as DTBT was designed and synthesized. DTBT-based conjugated polymers have been well investigated as photovoltaic materials, and seven representatives are shown in Scheme 2.7. The basic information of these polymers is listed in Table 2.2. It can be seen that the band gaps and as well the HOMO and LUMO levels of polymers were influenced by the electron donating properties of the building blocks. For example, in those seven building blocks, DTP is more electron-rich than the others, and hence the polymer PDTPDTBT exhibited much lower band gap and higher HOMO level than the rest [38]; fluorene unit is the weakest electron donating effect compared to the other building blocks, and therefore, its HOMO level reached −5.5 eV, the lowest one in these DTBT-based polymers [39]. All of these DTBT polymers exhibited very potential photovoltaic properties, and 5–7 % of PCEs have been achieved based on them and some interesting phenomena have been reveals. For instance, V_{oc} values of PFDTBT [39], PCDTBT [40, 41], and PFSiDTBT [42, 43]—based devices were 1, 0.9 and 0.88 V, respectively, which are among the highest values in OPV cells.

2.2.1.3 Pyrrolo[3,4-c]pyrrole-1,4-dione (DPP) Derivatives

DPP and its derivatives, usually have strong absorption bands in the visible range. Thiophene-based DPP derivatives have well-confined conjugated structures, and exhibit good charge-carrier mobilities for both holes and electrons. One of the first

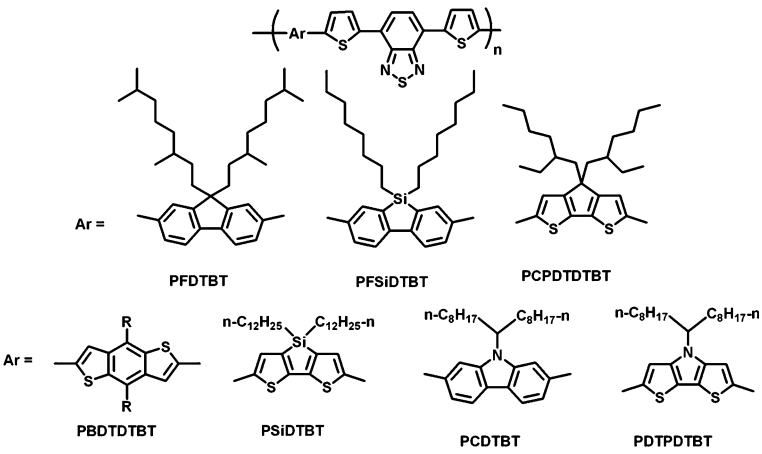

Scheme 2.7 Several representatives of DTBT-based polymers with D/A structure

organic electronic applications for DPP-based polymers was in ambipolar organic FETs. A DPP-based polymer having a mobility of 0.1 $cm^2\ V^{-1}\ s^{-1}$ for both holes and electrons were reported by Winnewisser et al. [44]. On the other hand, the DPP core can be synthesized easily with good yield (see Scheme 2.8). Therefore, DPP-based polymers and small molecular materials attracted much attention and more and more DPP-based photovoltaic materials have been developed in the recent years.

A large number of low band gap polymers have been synthesized since 2008, with the DPP unit and some of them are shown in Scheme 2.8 and their basic properties are listed in Table 2.3. The homopolymer (PDPP) was synthesized through Yamamoto coupling polymerization [45]. The band gap of this polymer is very low (1.24 eV). Moreover, the polymer is stable under ambient condition due to its low-lying HOMO level. However, the PCE of PDPP/PCBM-based solar cell was only 0.3 %. One of the main reasons given by the authors is the energy difference between the LUMO of the donor and the LUMO of the acceptor, which is only 0.18 eV [46, 47]. To extend the conjugation of the backbone, a third thiophene was added as shown in PTDPP. The polymerization was performed via a Suzuki cross-coupling polymerization, using 2,5-thiophenebis(boronic ester) as monomer [48]. The band gap of PTDPP was ~1.30 eV, and a PCE of 4.7 % was recorded (Scheme 2.9).

DPP was also copolymerized with the other commonly used conjugated components. It is worthy to mention that in comparison with DTBT-based polymers, DPP-based polymers possess much lower band gaps. For example, band gap of PFDPP and PCZDPP are 1.77 and 1.57 eV [45, 49], respectively, which are lower than their DTBT-based counterparts (PFDTBT and PCDTBT). Not only DPP-

Scheme 2.8 Synthesis of the DPP core

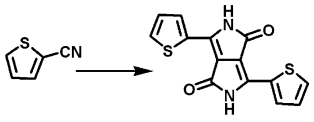

Table 2.3 Polymer properties and device characteristics for the DPP-based polymers

Polymer	Eg(opt) (eV)	HOMO/LUMO (eV/eV)	J_{sc} (mA/cm^2)	V_{oc} (V)	FF	PCE (%)	Refs
PTDPP	1.30	−5.17/− 3.16	11.8	0.65	0.60	4.7	[48]
PFDPP	1.77	−5.43/− 3.67	2.41	0.91	0.41	0.9	[45]
PCPDTDPP	1.39	−5.25/− 3.74	5.73	0.61	0.49	1.7	[45]
PPDTDPP	1.40	−5.10/− 3.40	11.3	0.61	0.58	4.0	[50]
PPPDPP	1.53	−5.35/− 3.53	10.8	0.80	0.65	5.5	[51]
PDPP	1.24	−5.29/− 3.99	0.76	0.64	0.58	0.3	[45]
PCZDPP	1.57	−5.44/− 3.92	8.6	0.80	0.47	3.2	[49]
PFGeDPP	1.63	−5.38/− 3.70	4.10	0.76	0.62	1.5	[52]
PTPDDPP	1.13	−4.90/− 3.63	14.9	0.38	0.48	2.7	[53]
PBDTDPP	1.43	−5.15/− 3.69	6.72	0.74	0.56	2.8	[54]

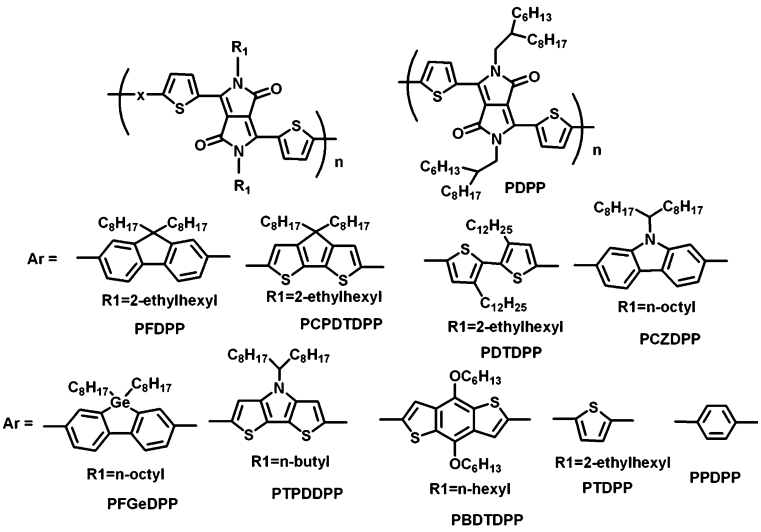

Scheme 2.9 Molecular structures of DPP-based polymers

based polymers, but also DPP-based small molecular compounds exhibited very potential photovoltaic properties. For instance, several solution-processable DPP-based small molecules (1.5−1.8 eV) with PCEs better than 4 % have been reported.

2.2.1.4 Benzo[1,2-b;4,5-b′]dithiophene-Based Polymers

As reported, three kinds of functional groups, including alkoxy, alkyl, and alkylthiophene, were used as side groups on the 4- and 8-positions of the BDT unit to make solution-processable polymers. The alkoxy-substituted BDT can be synthesized easily through a one-pot two-step reaction [55]. Typically, the yield of the alkoxy substituted BDT was between 70 and 90 %. The alkyl-substituted BDT compounds can be synthesized by the three-step reaction as reported [56]. The alkylthiophene-substituted BDT compounds were synthesized by the similar reaction for alkynyl-substituted BDTs, but 2-lithium-5-alkyl-thiophene was used instead of alkynyl lithium [57]. BDT has a symmetric and planar conjugated structure, and hence tight and regular stacking can be expected for the BDT-based conjugated polymers. Therefore, BDT-based polymers were first used in organic field effect transistors (OFETs). In 2007, a BDT-thiophene-based polymer was reported and exhibited a hole mobility of 0.25 $cm^2\ V^{-1}\ s^{-1}$, which was one of the highest values for polymer-based OFET [58] (Scheme 2.10).

Band gap and molecular energy level of BDT-based polymers can be readily tuned in a wide range by copolymerizing with conjugated building blocks with different electron withdrawing effect. Hou et al., first designed and synthesized

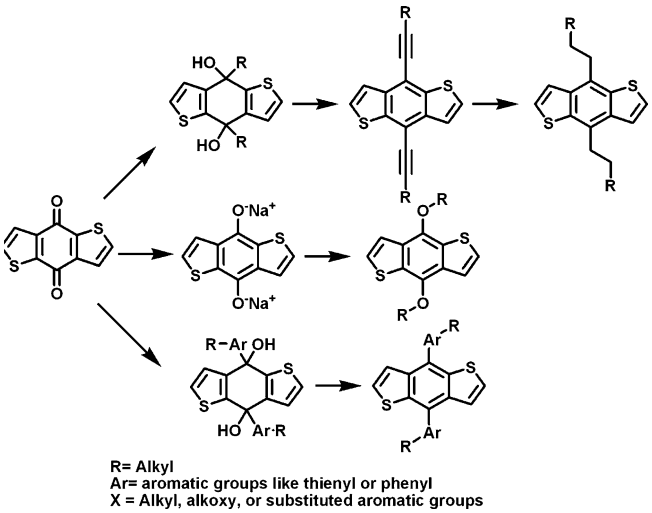

Scheme 2.10 Synthesis of three kinds of substituted BDTs

eight BDT-based polymers, as shown in Scheme 2.11, to investigate the correlation among conjugated backbones, band gaps, and molecular energy levels [59]. Furthermore, the correlation between HOMO levels of those polymers and the V_{oc} values of the devices based on them were also studied in this work. It can be seen that V_{oc} of the devices was directly proportional to the offset between HOMO level of the electron donor material and LUMO level of PCBM. Although, the polymer PBDTTPZ exhibited strong and broad absorption band, but V_{oc} of the PBDTTPZ/PCBM-based device was only 0.2 V due to the high-lying HOMO level of the polymer, meaning that the balance between band gap and HOMO level would be of great importance to the molecular structure design Fig. 2.2.

In the mean time, more and more BDT-based polymers were designed, synthesized, and applied in PSCs. The BDT derivatives were copolymerized with many kinds of building blocks, like derivatives of thiophene, BT and the likes,

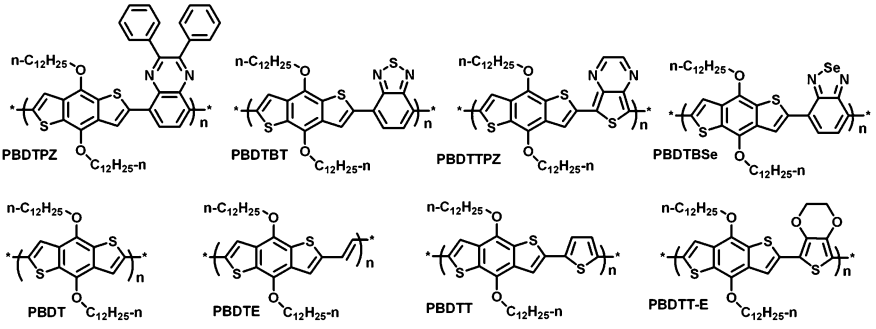

Scheme 2.11 Eight BDT-based polymers with identical BDT moieties

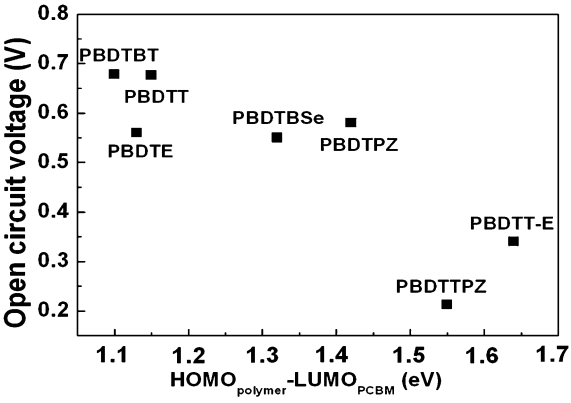

Fig. 2.2 Open-circuit voltage distribution of the devices based on BDT polymers; average values are shown as *squares*

imides and diimide-containing conjugated components. These polymers made great success in PSCs. Molecular structures of several highly efficient BDT-based photovoltaic materials (PCE = ~7 %) were shown in Scheme 2.12, and their basic properties were listed in Table 2.4.

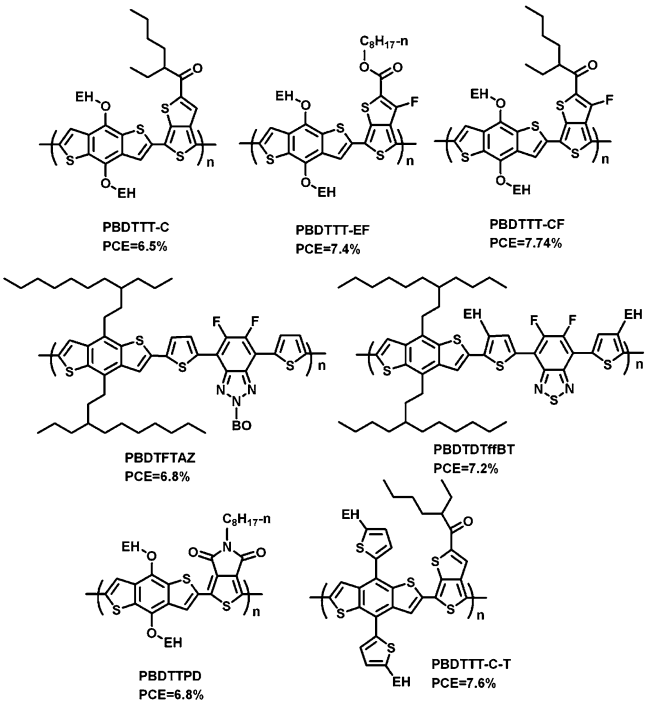

Scheme 2.12 Molecular structures of BDT-based polymers with PCE ~7 %

Table 2.4 Properties and devices characteristics for the BDT-based low band gap polymers

Polymer	Eg(opt) (eV)	HOMO/LUMO (eV/eV)	J_{sc} (mA/cm^2)	V_{oc} (V)	FF	PCE (%)	Refs
PBDT	2.13	−5.16/− 2.67	N.A.	N.A.	N.A.	N.A.	[59]
PBDTE	2.03	−5.07/− 2.86	1.16	0.56	0.38	0.25	[59]
PBDTT	2.06	−5.05/− 2.69	3.78	0.75	0.56	1.60	[59]
PBDTT-E	1.97	−4.56/− 2.66	2.46	0.37	0.40	0.36	[59]
PBDTPZ	1.63	−4.78/− 3.28	1.54	0.60	0.26	0.23	[59]
PBDTBT	1.70	−5.10/–3.19	2.97	0.68	0.44	0.90	[59]
PBDTTPZ	1.05	−4.65/− 3.46	1.41	0.22	0.35	0.11	[59]
PBDTBSe	1.52	−4.88/− 3.33	1.05	0.55	0.32	0.18	[59]
PBDTTT-C	1.61	−5.12/− 3.35	14.7	0.70	0.64	6.58	[14]
PBDTTT-CF	1.60	−5.22/− 3.45	15.2	0.76	0.67	7.73	[15]
PBDTTT-EF	1.63	−5.12/− 3.13	14.5	0.74	0.69	7.4	[60]
PBDTTTPD	1.73	−5.40/N.A.	11.5	0.85	0.70	6.8	[61]
PBDTFTAZ	2.0	−5.36/− 3.05	11.8	0.79	0.73	6.81	[62]
PBDTDTffBT	1.70	−5.54/− 3.33	12.91	0.91	0.61	7.2	[63]
PBDTTT-C-T	1.58	−5.11/− 3.25	17.48	0.74	0.59	7.59	[57]

2.2.2 Electron Acceptors

Organic materials with appropriate properties, including conjugated polymers and small molecular compounds, can be used as electron donor materials in OPV. Many organic compounds exhibited potential properties as electron acceptor material, but only a very few electron acceptor materials can be used in highly efficient OPV devices. Fullerene and its derivatives are the most successful electron acceptor materials.

2.2.2.1 PCBM and the Likes

Fullerene C60 has well-symmetric structure and exhibits good electron mobility, and as known, one molecule of C60 can receive four electrons. Therefore, C60 and its derivatives can be used as electron acceptor materials. In 1992, Sariciftci et al. first used C60 as electron acceptor and discovered the photoinduced ultrafast electron transfer between electron donor and acceptor [64]. Although, C60 can be dissolved in CB and DCB, it exhibits very limited solubility in most of the commonly used organic solvents. In order to improve its solubility and also to avoid severe phase separation of D/A blend, [6,6]-phenyl-C61-butyric acid methyl ester ($PC_{60}BM$) was applied in OPVs. In the past decade, $PC_{60}BM$ and its corresponding C70 derivative ($PC_{70}BM$) has been dominantly used as acceptors in OPVs. In comparison with $PC_{60}BM$, $PC_{70}BM$ possesses stronger absorption in visible range, and hence it attracted much interest recently. However, C70 is much expensive than that of C60 due to its tedious purification process, which limits its application. The molecular structures and the synthetic route of $PC_{60}BM$, $PC_{70}BM$

are shown in Scheme 2.13. $PC_{60}BM$ was crystalline dark-brown powder, and possesses good solubility in common organic solvents such as chloroform, toluene, and *o*-dichlorobenzene [65].

Absorption spectra of PC60BM and PC70BM are shown in Fig. 2.3. It can be seen that both the two materials show strong absorption at ultraviolet region, from 200 to 400 nm, but PC70BM shows stronger absorption in visible region compared to PC60BM. Since, OPV devices using PC70BM as acceptor will harvest more sunlight, many OPVs using PC70BM as acceptor show bigger J_{sc} and hence better PCEs than that of PC60BM-based devices.

The electrochemical properties and energy level of the fullerene derivatives is very important for PSCs. The open-circuit voltage (V_{oc}) of PSCs is determined by the difference between the LUMO energy level of the fullerene acceptors and the HOMO energy level of the polymer donors [66, 67]. Therefore, the LUMO energy level of the fullerene derivatives is a key parameter for the application of an acceptor to match with a polymer donor. LUMO level of electron donors or acceptors can be measured by cyclic voltammogram (CV) method. LUMO level of unsubstituted C60 and PCBM were ~ -4.2 and -4.0 eV, respectively [68, 69]. Based on the difference of the LUMO levels of those two compounds, it is easy to conclude that LUMO level of C60 can be elevated by adding the substituent. As discussed in the above section, higher LUMO level of electron acceptor materials would be helpful to get higher V_{oc}, and for the purpose to get higher LUMO level, the bisadducts and multiadducts of fullerene were used in OPVs. For example, the LUMO level of bis-PCBM was 0.1–0.15 eV higher than that of PCBM, and when bis-PCBM was used as electron acceptor in P3HT-based OPV device, a V_{oc} of 0.72 V was recorded, which was 0.12 V higher than the PCBM/P3HT-based devices [70]. Furthermore, multiadducts can also be used in OPVs, and higher V_{oc} of the device can be realized. However, since the substituent of PCBM is inert for electron transport and the symmetric property of fullerene can be weakened, electron transport properties of the bis- or multiadducts were not as good as that of PCBM. Therefore, PC60BM and PC70BM are still among the best electron acceptors in OPVs. The photovoltaic properties of the fullerene derivatives were studied by fabricating the PSCs based on P3HT as donor and the fullerene derivatives as acceptor, and the results are listed in Table 2.5 [70–72] Scheme 2.14.

Scheme 2.13 Molecular structures of $PC_{60}BM$ and $PC_{70}BM$

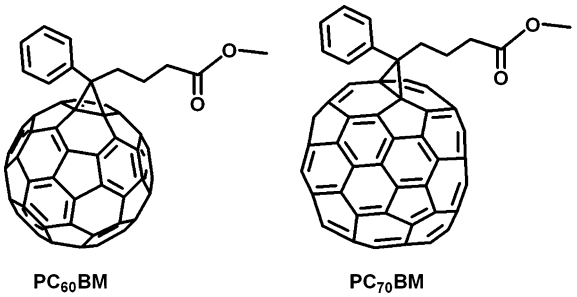

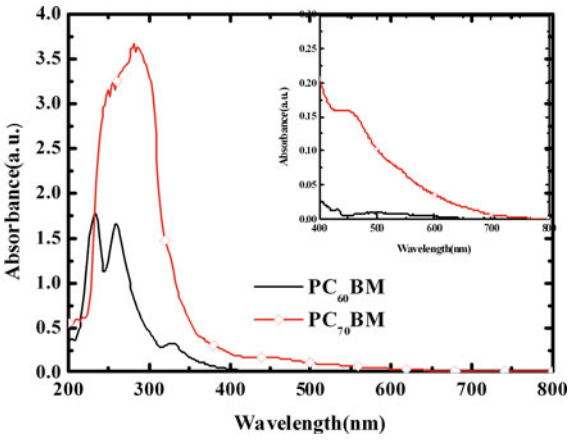

Fig. 2.3 Absorption spectra of $PC_{60}BM$ and $PC_{70}BM$

Table 2.5 Photovoltaic performance of the fullerene multiadduct acceptors

Donor/acceptor (weight ratio)	J_{sc} (mA/cm^2)	V_{oc} (V)	FF	PCE (%)	Refs
P3HT/$PC_{60}BM$(1:0.8)	10.9	0.62	0.62	4.18	[72]
P3HT/bis$ThC_{60}BM$(1:1.2)	5.91	0.72	0.41	1.73	[72]
P3HT/tri$ThC_{60}BM$(1:1.4)	1.88	0.64	0.28	0.34	[72]
P3HT/bis$PC_{60}BM$(1:1.2)	9.14	0.724	0.68	4.5	[71]
P3HT/$PC_{60}BM$(1:1)	8.94	0.61	0.60	2.4	[70]
P3HT/bis$PC_{60}BM$(1:1.2)	7.30	0.73	0.63	2.4	[70]
P3HT/bis$PC_{70}BM$(1:1.2)	7.03	0.75	0.62	2.3	[70]
P3HT/bis$ThC_{60}BM$(1:1.2)	7.31	0.72	0.66	2.5	[70]

2.2.2.2 Indene-C_{60} Bisadduct and Indene-C_{70} Bisadduct (ICBA)

Indene-fullerene adducts were used as electron acceptor materials in OPVs [73–75]. This kind of compounds can be synthesized easily by a one-pot reaction. The solution of indene and fullerene (C60 or C70) in DCB was heated to reflux for several hours, and a mixture of unreacted fullerene, indene-fullerene monoadduct (ICMA), indene-fullerene bisadduct (ICBA), and indene-fullerene multiadduct can be obtained, which can be separated readily through column chromatography. LUMO levels of ICMA and ICBA are −3.86 and −3.74 eV respectively [73]; both are higher than that of PCBM, and thus ICMA/P3HT- and ICBA/P3HT-based devices showed higher V_{oc} than that of P3HT/PCBM-based devices. ICMA has poor solubility in CB or DCB, which limits the photovoltaic performance of the devices; ICBA can be easily dissolved into CB or DCB, and its LUMO level was higher than ICMA and PCBM.

ICBA was successfully used in P3HT-based solar cells. Typically, V_{oc} of P3HT/PCBM system is ~0.6 V; in P3HT/ICBA system, V_{oc} of 0.84 V can be obtained without sacrificing the other parameters, including FF and J_{sc}. The great increase on V_{oc} should be benefited from the high-lying LUMO of ICBA. The

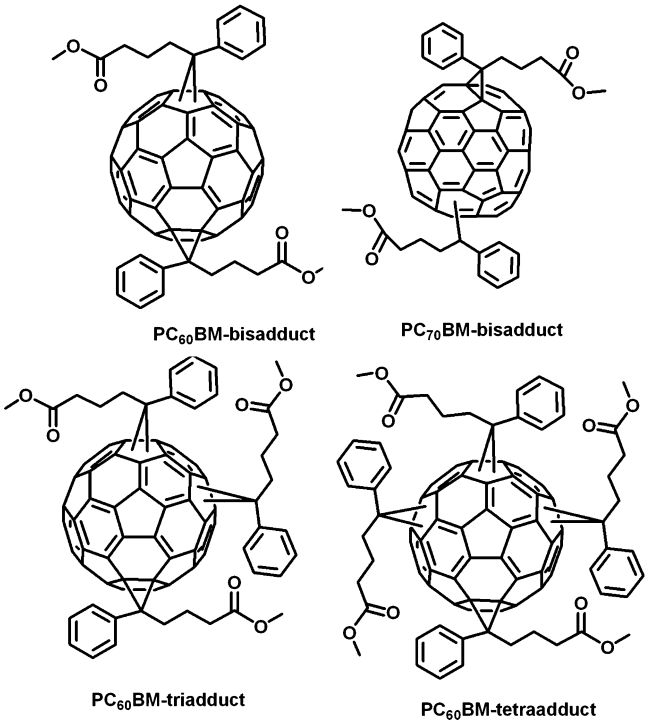

Scheme 2.14 Molecular structures of fullerene multiadduct derivatives

PCE values of the PSCs based on P3HT/IC60BA and P3HT/IC70BA reached 5.44 and 5.64 %, respectively [73, 75], which is more than 40 % increased in comparison with that of the PSCs based on P3HT/PC60BM. After further device optimization, the PSCs based on P3HT/IC60BA displayed a V_{oc} of 0.84 V, a J_{sc} of 10.61 mA cm^{-2}, a FF of 72.7 %, and a PCE of 6.48 % [74]. The photovoltaic properties of the fullerene derivatives were studied by fabricating the PSCs based on P3HT as donor and the fullerene derivatives as acceptor, and the results are listed in Table 2.6 [73–75] Scheme 2.15.

2.2.2.3 Other Fullerenes

In addition to the above-mentioned fullerene derivative acceptors, there are some other fullerene derivatives for application as acceptors in PSCs reported in literature. Such as PC84BM [76] and endohedral fullerenes [77] and so on.

Table 2.6 Photovoltaic performance of the fullerene multiadduct acceptors

Donor/acceptor (weight ratio)	I_{sc} (mA/cm^2)	V_{oc} (V)	FF	PCE (%)	Refs
P3HT/$PC_{60}BM$(1:1)	10.8	0.58	0.62	3.88	[73]
P3HT/$IC_{60}MA$(1:1)	9.66	0.63	0.64	3.89	[73]
P3HT/$IC_{60}BA$(1:1)	9.67	0.84	0.67	5.44	[73]
P3HT/$IC_{60}BA$(1:1)	10.61	0.84	0.73	6.48	[74]
P3HT/$IC_{70}BA$(1:1)	9.73	0.84	0.69	5.64	[75]

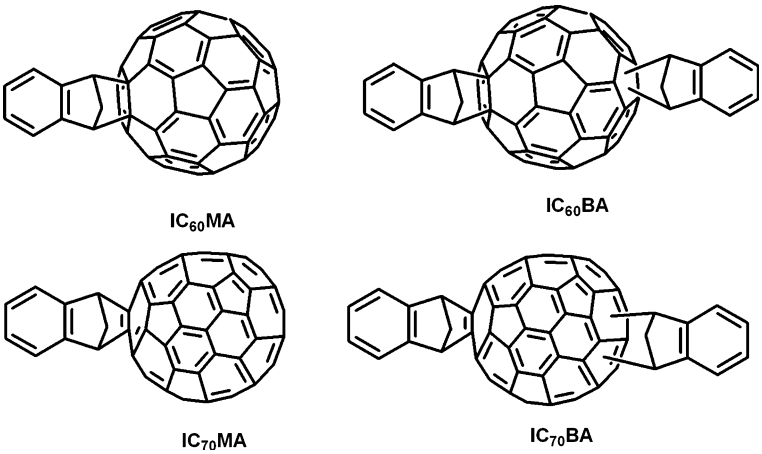

Scheme 2.15 Molecular structures of indene-fullerene adducts

2.3 Conclusion

In the past two decades, a number of organic photovoltaic materials have been designed, synthesized, and applied in OPVs. Although, PCE of OPV cells has been reached over 8 %, the development of active layer materials is still the key to boost the efficiency. In order to get better photovoltaic properties, many properties, like band gap, molecular energy level, mobility, solubility, etc., should be considered, and how to balance these parameters is the most important part to molecular design.

References

1. Yu G, Gao J, Hummelen JC, Wudl F, Heeger AJ (1995) Polymer photovoltaic cells: enhanced efficiencies via a network of internal donor-acceptor heterojunctions. Science 270:1789–1791. doi:10.1126/science.270.5243.1789
2. Scharber MC, Muhlbacher D, Koppe M, Denk P, Waldauf C, Heeger AJ, Brabec CJ (2006) Design rules for donors in bulk-heterojunction solar cells—towards 10% energy-conversion efficiency. Adv Mater 18:789–794. doi:10.1002/adma.200501717

3. Osaka I, Mccullough RD (2008) Advances in molecular design and synthesis of regioregular polythiophenes. Acc Chem Res 41:1202–1214. doi:10.1021/ar800130s
4. Chen MH, Hou JH, Hong Z, Yang G, Sista S, Chen LM, Yang Y (2009) Efficient polymer solar cells with thin active layers based on alternating polyfluorene copolymer/fullerene bulk heterojunctions. Adv Mater 21:4238–4242. doi:10.1002/adma.200900510
5. Shrotriya V, Wu EHE, Li G, Yao Y, Yang Y (2006) Efficient light harvesting in multiple-device stacked structure for polymer solar cells. Appl Phys Lett 88:064104. doi:10.1063/1.2172741
6. Shaheen SE, Brabec CJ, Sariciftci NS, Padinger F, Fromherz T, Hunnelen JC (2001) 2.5% Efficient organic plastic solar cells. Appl Phys Lett 78:841–843. doi:10.1063/1.1345834
7. Ma WL, Yang CY, Gong X, Lee KH, Heeger A (2005) Thermally stable, efficient polymer solar cells with nanoscale control of the interpenetrating network morphology. Adv Funct Mater 15:1617–1622. doi:10.1002/adfm.200500211
8. Moulé AJ, Meerholz K (2008) Controlling morphology in polymer–fullerene mixtures. Adv Mater 20:240–245. doi:10.1002/adma.200701519
9. Li G, Shrotriva V, Huang JS, Yao Y, Moriarty T, Emery K, Yang Y (2005) High-efficiency solution processable polymer photovoltaic cells by self-organization of polymer blends. Nat Mater 4:864–868. doi:10.1038/nmat1500
10. Zhao Y, Xie ZY, Qu Y, Geng YH, Wang L (2007) Organic light emitting device having multiple separate emissive layers. Appl Phys Lett 90: 043504-1–3. doi:10.1063/1.2434173
11. Peet J, Kim JY, Coates NE, Ma WL, Heeger AJ, Moses D, Bazan GC (2007) Efficiency enhancement in low-bandgap polymer solar cells by processing with alkane dithiols. Nat Mater 6:497–500. doi:10.1038/nmat1928
12. Bredas JL (1985) Relationship between band gap and bond length alternation in organic conjugated polymers. J Chem Phys 82:3808–3811. doi:10.1063/1.448868
13. Liang YY, Feng DQ, Wu Y, Tsai ST, Li G, Ray C, Yu LP (2009) Highly efficient solar cell polymers developed via fine-tuning of structural and electronic properties. J Am Chem Soc 131:7792–7799. doi:10.1021/ja901545q
14. Hou JH, Chen HY, Zhang SQ, Chen RI, Yang Y, Wu Y, Li G (2009) Synthesis of a Low Band Gap Polymer and Its Application in Highly Efficient Polymer Solar Cells. J Am Chem Soc 131:5586–15587. doi:10.1021/ja9064975
15. Chen HY, Hou JH, Zhang SQ, Liang YY, Yang GW, Yang Y, Yu LP, Wu Y, Li G (2009) Polymer solar cells with enhanced open-circuit voltage and efficiency. Nat Photon 3:649–653. doi:10.1038/nphoton.2009.192
16. Huang Y, Huo LJ, Zhang SQ, Guo X, Han C, Li YF, Hou JH (2011) Sulfonyl: a new application of electron-withdrawing substituent in highly efficient photovoltaic polymer. Chem Commun 47:8904–8906. doi:10.1039/C1CC12575C
17. Sato M, Morii H (1991) Polym Commun 32:42–44
18. Hou JH, Tan ZA, Yan Y, He YJ, Yang CH, Li YF (2006) Synthesis and photovoltaic properties of two-dimensional conjugated polythiophenes with bi(thienylenevinylene) side chains. J Am Chem Soc 128:4911–4916. doi:10.1021/ja060141m
19. Zhou EJ, Tan Z, Yang Y, Huo LJ, Zou YP, Yang CH, Li YF (2007) Synthesis, hole mobility, and photovoltaic properties of cross-linked polythiophenes with vinylene-terthiophene-vinylene as conjugated bridge. Macromolecules 40:1831–1837. doi:10.1021/ma062633p
20. Hou JH, Chen TL, Zhang SQ, Huo LJ, Sista S, Yang Y (2009) An easy and effective method to modulate molecular energy level of poly(3-alkylthiophene) for high voc polymer solar cells. Macromolecules 42:9217–9219. doi:10.1021/ma902197a
21. Ballantyne AM, Chen L, Nelson J, Bradley DDC, Astuti Y, Maurano A, Shuttle CG, Durrant JR, Heeney M, Duffy W, McCulloch I (2007) Studies of highly regioregular poly(3-hexylselenophene) for photovoltaic applications. Adv Mater 19:4544–4547. doi:10.1002/adma.200701265
22. Muhlbacher D, Scharber M, Morana M, Zhu Z, Waller D, Gaudiana R, Brabec C (2006) High photovoltaic performance of a low-bandgap polymer. Adv Mater 18:2884–2889. doi:10.1002/adma.200600160

23. Tsao HN, Cho D, Andreasen JW, Rouhanipour A, Breiby DW, Pisula W, Mullen K (2009) The influence of morphology on high-performance polymer field-effect transistors. Adv Mater 21:209–212. doi:10.1002/adma.200802032
24. Coffin RC, Peet J, Rogers J, Bazan GC (2009) Streamlined microwave-assisted preparation of narrow-bandgap conjugated polymers for high-performance bulk heterojunction solar cells. Nat Chem 1:657–661. doi:10.1038/NCHEM.403
25. Zhu ZG, Waller D, Gaudiana R, Morana M, Mühlbacher D, Scharber M, Brabec C (2007) Panchromatic conjugated polymers containing alternating donor/acceptor units for photovoltaic applications. Macromolecules 40:1981–1986. doi:10.1021/ma062376o
26. Peet J, Kim JY, Coates NE, Ma WL, Moses D, Heeger AJ, Bazan GC (2007) Efficiency enhancement in low-bandgap polymer solar cells by processing with alkane dithiols. Nat Mater 6:497–500. doi:10.1038/nmat1928
27. Su MS, Kuo CY, Yuan MC, Jeng US, Su CJ, Wei KH (2011) Improving device efficiency of polymer/fullerene bulk heterojunction solar cells through enhanced crystallinity and reduced grain boundaries induced by solvent additives. Adv Mater 23:3315–3319. doi:10.1002/adma.201101274
28. Hou J, Chen HY, Zhang S, Li G, Yang Y (2008) Synthesis, characterization, and photovoltaic properties of a low band gap polymer based on silole-containing polythiophenes and 2,1,3-benzothiadiazole. J Am Chem Soc 130:16144–16145. doi:10.1021/ja806687u
29. Chen HY, Hou J, Hayden AE, Yang H, Houk KN, Yang Y (2010) Silicon atom substitution enhances interchain packing in a thiophene-based polymer system. Adv Mater 22:371–375. doi:10.1002/adma.200902469
30. Yue W, Zhao Y, Shao S, Tian H, Xie Z, Geng Y, Wang F (2009) Novel NIR-absorbing conjugated polymers for efficient polymer solar cells: effect of alkyl chain length on device performance. J Mater Chem 19:2199–2206. doi:10.1039/b818885h
31. Chen MH, Hou J, Hong Z, Yang G, Sista S, Chen LM, Yang Y (2009) Efficient polymer solar cells with thin active layers based on alternating polyfluorene copolymer/fullerene bulk heterojunctions. Adv Mater 21:4238–4242. doi:10.1002/adma.200900510
32. Wang E, Wang L, Lan L, Luo C, Zhuang W, Peng J, Cao Y (2008) High-performance polymer heterojunction solar cells of a polysilafluorene derivative. Appl Phys Lett 92: 033307-1–3. doi:10.1063/1.2836266
33. Blouin N, Michaud A, Gendron D, Wakim, Blair E, Neagu-Plesu R, Belletete M, Durocher G, Tao Y, Leclerc M (2008) Toward a rational design of poly(2,7-carbazole) derivatives for solar cells. J Am Chem Soc 130:732–733. doi:10.1021/ja0771989
34. Zhou EJ, Nakamura M, Nishizawa T, Zhang Y, Wei QS, Tajima K, Yang CH, Hashimoto K (2008) Synthesis and photovoltaic properties of a novel low band gap polymer based on n-substituted dithieno[3,2-b:2′,3′-d]pyrrole. Macromolecules 41:8302–8305. doi:10.1021/ma802052w
35. Moulé J, Tsami A, Bünnagel TW, Forster M, Kronenberg NM, Scharber M, Koppe M, Morana M, Brabec CJ, Meerholz K, Scherf U (2008) Two novel cyclopentadithiophene-based alternating copolymers as potential donor components for high-efficiency bulk-heterojunction-type solar cells. Chem Mater 20:4045–4050. doi:10.1021/cm8006638
36. Huo LJ, Hou JH, Zhang SQ, Chen HY, Yang YA (2010) Polybenzo[1,2-b:4,5-b′]dithiophene derivative with deep homo level and its application in high-performance polymer solar cells. Angew Chem Int Ed 49:1500–1503. doi:10.1002/anie.200906934
37. Huo LJ, Guo X, Li YF, Hou JH (2011) Synthesis of a polythieno[3,4-b]thiophene derivative with a low-lying HOMO level and its application in polymer solar cells. Chem Commun 47:8850–8852. doi:10.1039/c1cc12643a
38. Liu J, Zhang R, Sauve G, Kowalewski T, McCullough RD (2008) Highly disordered polymer field effect transistors: n-alkyl dithieno[3,2-b:2',3'-d]pyrrole-based copolymers with surprisingly high charge carrier mobilities. J Am Chem Soc 130:13167–13176. doi:10.1021/ja803077v

39. Slooff LH, Veenstra SC, Kroon JM, Moet DJD, Sweelssen J, Koetse MM (2007) Determining the internal quantum efficiency of highly efficient polymer solar cells through optical modeling. Appl Phys Lett 90: 143506-1–3. doi:10.1063/1.2718488
40. Blouin N, Michaud A, Leclerc M (2007) A low-bandgap poly(2,7-carbazole) derivative for use in high-performance solar cells. Adv Mater 19:2295–2300. doi:10.1002/adma.200602496
41. Blouin N, Michaud A, Gendron D, Wakim S, Blair E, Neagu-Plesu R, Belletete M, Durocher G, Tao Y, Leclerc M (2008) Toward a rational design of poly(2,7-carbazole) derivatives for solar cells. J Am Chem Soc 130:732–742. doi:10.1021/ja0771989
42. Boudreault PLT, Michaud A, Leclerc MA (2007) New poly(2,7-dibenzosilole) derivative in polymer solar cells. Macromol Rapid Commun 28:2176–2179. doi:10.1002/marc.200700470
43. Wang E, Wang L, Lan L, Luo C, Zhuang W, Peng J, Cao Y (2008) High-performance polymer heterojunction solar cells of a polysilafluorene derivative. Appl Phys Lett 92:033307-1–3. doi:10.1063/1.2836266
44. Burgi L, Turbiez M, Pfeiffer R, Bienewald F, Kirner HJ, Winnewisser C (2008) High-mobility ambipolar near-infrared light-emitting polymer field-effect transistors. Adv Mater 20:2217–2224. doi:10.1002/adma.200702775
45. Zoombelt AP, Mathijssen SGJ, Turbiez MGR, Wienk MM, Janssen RAJ (2010) Small band gap polymers based on diketopyrrolopyrrole. J Mater Chem 20:2240–2246. doi:10.1039/b919066j
46. Zoombelt AP, Fonrodona M, Wienk MM, Sieval AB, Hummelen JC, Janssen RA (2009) Photovoltaic performance of an ultrasmall band gap polymer. J Org Lett 11:903–906. doi:10.1021/ol802839z
47. Zoombelt AP, Fonrodona M, Turbiez MGR, Wienk MM, Janssen RAJ (2009) Synthesis and photovoltaic performance of a series of small band gap polymers. J Mater Chem 19:5336–5342. doi:10.1039/b821979f
48. Bijleveld JC, Zoombelt AP, Mathijssen SGJ, Wienk MM, Turbiez M, de Leeuw DM, Janssen RAJ (2009) Poly(diketopyrrolopyrrole-terthiophene) for ambipolar logic and photovoltaics. J Am Chem Soc 131:16616–16617. doi:10.1021/ja907506r
49. Zou YP, Gendron D, Aich RB, Najari A, Tao Y, Leclerc M (2009) High-mobility low-bandgap poly(2,7-carbazole) derivative for photovoltaic. applications. Macromolecules 42:2891–2894. doi:10.1021/ma900119x
50. Wienk MM, Turbiez M, Gilot J, Janssen RA (2008) Narrow-bandgap diketo-pyrrolo-pyrrole polymer solar cells: the effect of processing on the performance. J Adv Mater 20:2556–2560. doi:10.1002/adma.200800456
51. Bijleveld JC, Gevaerts VS, Di Nuzzo D, Turbiez M, Mathijssen SGJ, de Leeuw DM, Wienk MM, Janssen RAJ (2010) Efficient solar cells based on an easily accessible diketopyrrolopyrrole polymer. Adv Mater 22:E242–E246. doi:10.1002/adma.201001449
52. Allard N, Aich RB, Gendron D, Boudreault PLT, Tessier C Alem S, Tse SC, Tao Y, Leclerc M (2010) Germafluorenes: new heterocycles for plastic electronics. Macromolecules 43:2328–2333. doi:10.1021/ma9025866
53. Zhou E, Wei Q, Yamakawa S, Zhang Y, Tajima K, Yang C, Hashimoto K (2010) Diketopyrrolopyrrole-based semiconducting polymer for photovoltaic device with photocurrent response wavelengths up to 1.1 μm. Macromolecules 43:821–826. doi:10.1021/ma902398q
54. Kanimozhi C, Balraju P, Sharma GD, Patil S (2010) Synthesis of diketopyrrolopyrrole containing copolymers: a study of their optical and photovoltaic properties. J Phys Chem B 114:3095–3103. doi:10.1021/jp909183x
55. Hou J, Park MH, Zhang S, Yao Y, Chen LM, Li JH, Yang Y (2008) Bandgap and molecular energy level control of conjugated polymer photovoltaic materials based on benzo[1,2-b:4,5-b′]dithiophene. Macromolecules 41:6012–6018. doi:10.1021/ma800820r
56. Pan H, Li Y, Wu Y, Liu P, Ong BS, Zhu S, Xu G (2006) Synthesis and thin-film transistor performance of poly(4,8-didodecylbenzo[1,2-b:4,5-b′]dithiophene. Chem Mater 18:3237–3241. doi:10.1021/cm0602592

57. Huo LJ, Zhang SQ, Guo X, Xu F, Li YF, Hou JH (2011) Replacing alkoxy groups with alkylthienyl groups: a feasible approach to improve the properties of photovoltaic polymers. Angew Chem Int Ed 50:9697–9702. doi:10.1002/anie.201103313
58. Pan H, Li Y, Wu Y, Liu P, Ong BS, Zhu S, Xu G (2007) Low-temperature, solution-processed, high-mobility polymer semiconductors for thin-film transistors. J Am Chem Soc 129:4112–4113. doi:10.1021/ja067879o
59. Hou JH, Park MH, Zhang SQ, Yao Y, Chen LM, Li JH, Yang Y (2008) Bandgap and molecular energy level control of conjugated polymer photovoltaic materials based on benzo[1,2-b:4,5-b′]dithiophene. Macromolecules 41:6012–6018. doi:10.1021/ma800820r
60. Liang YY, Yu LP (2010) A new class of semiconducting polymers for bulk heterojunction solar cells with exceptionally high performance. Acc Chem Res 43:1227–1236. doi:10.1021/ar1000296
61. Piliego C, Holcombe TW, Douglas JD (2010) Synthetic Control of Structural Order in N-Alkylthieno[3,4-c]pyrrole-4,6-dione-Based Polymers for Efficient Solar Cells. J Am Chem Soc 132:7595–7597. doi:10.1021/ja103275u
62. Price SC, Stuart AC, Yang LQ (2011) Fluorine substituted conjugated polymer of medium band gap yields 7% efficiency in polymer—fullerene solar cells. J Am Chem Soc 133:4625–4631. doi:10.1021/ja1112595
63. Zhou HX, Yang LQ, Stuart AC (2011) Development of fluorinated benzothiadiazole as a structural unit for a polymer solar cell of 7% efficiency. Angew Chem Int Ed 50:2995–2998. doi:10.1002/anie.201005451
64. Sariciftci NS, Smilowitz L, Heeger AJ, Wudl F (1992) Photoinduced electron transfer from a conducting polymer to buckminsterfullerene. Science 258:1474–1476. doi:10.1126/science.258.5087.1474
65. Hummelen JC, Knight BW, Lepeq F, Wudl F (1995) Preparation and characterization of fulleroid and methanofullerene derivatives. J Org Chem 60:532–538. doi:10.1021/jo00108a012
66. Brabec CJ, Sariciftci NS, Hummelen JC (2001) Plastic solar cells. origin of the open circuit voltage of plastic solar cells. Adv Funct Mater 11:15–26. doi:1616-301X/01/0510-0379
67. Scharber MC, Wuhlbacher D, Koppe M (2006) Design rules for donors in bulk-heterojunction solar cells—towards 10% energy-conversion efficiency. Adv Mater 18:789–794. doi:10.1002/adma.200501717
68. Sariciftci NS, Braun D, Zhang C, Srdanov VI, Heeger AJ, Stucky G, Wudl F (1993) Semiconducting polymerbuckminsterfullerene heterojunctions: diodes, photodiodes, and photovoltaic cells. Appl Phys Lett 62:585–587. doi:10.1063/1.108863
69. He YJ, Li YF (2011) Fullerene derivative acceptors for high performance polymer solar cells. Phys Chem Chem Phys 13:1970–1983. doi:10.1021/ja103275u
70. Lenes M, Shelton SW, Sieval AB, Kronholm DF, Hummelen JC, Blom PWM (2009) Electron trapping in higher adduct fullerene-based solar cells. Adv Funct Mater 19:3002–3007. doi:10.1002/adfm.200900459
71. Lenes M, Wetzelaer G, Kooist FB, Veenstra SJJC, Blom PWM (2008) Fullerene bisadducts for enhanced open-circuit voltages and efficiencies in polymer solar cells. Adv Mater 20:2116–2119. doi:10.1002/adma.200702438
72. Choi JH, Son KI, Kim T, Kim K, Ohkubo K, Fukuzumi S (2010) Thienyl-substituted methanofullerene derivatives for organic photovoltaic cells. J Mater Chem 20:475–482. doi:10.1039/B916597E
73. He YJ, Chen HY, Hou JH, Li YF (2010) Indene—C60 bisadduct: a new acceptor for high-performance polymer solar cells. J Am Chem Soc 132:1377–1382. doi:10.1021/ja908602j
74. Zhao GJ, He YJ, Li YF (2010) 6.5% efficiency of polymer solar cells based on poly(3-hexylthiophene) and indene-C60 bisadduct by device optimization. Adv Mater 22:4355–4358. doi:10.1002/adma.201001339
75. He YJ, Zhao GJ, Peng B, Li YF (2010) High-yield synthesis and electrochemical and photovoltaic properties of indene-c70 bisadduct. Adv Funct Mater 20:3383–3389. doi:10.1002/adfm.201001122

76. Kooistra FB, Mihailetchi VD, Popescu LM, Kronholm D, Blom PWM, Hummelen JC (2006) New C84 derivative and its application in a bulk heterojunction. Solar Cell Chem Mater 18:3068–3073. doi:10.1021/cm052783z
77. Stevenson S, Rice G, Glass T, Harich K, Cromer F, Jordan MR, Craft J, Hadju E, Bible R, Olmstead MM, Maitra K, Fisher AJ, Balch A, Dorn HC (1999) Small-bandgap endohedral metallofullerenes in high yield and purity. Nature 401:55–57. doi:10.1038/43415